HIGHER EFFICIENCY FOR THIN MULTI CRYSTALLINE SILICON SOLAR CELLS BY IMPROVING THE REAR SURFACE PASSIVATION

C.J.J. Tool, P. Manshanden, A.R. Burgers, A.W. Weeber
ECN Solar Energy, PO BOX 1, 1755 ZG Petten, The Netherlands

ABSTRACT

For wafers thicker than 200 um, the efficiency of industrial multi crystalline silicon solar cells is independent of wafer thickness. An important efficiency limitation of these thin solar cells is the poor rear surface passivation due to the short minority carrier diffusion length of the aluminium BSF. The most likely reason for the poor quality of the BSF is the poor crystallinity of the BSF due to fast cooling of the cells during metallisation firing. Possible solutions to overcome this limitation are presented.

INTRODUCTION

Two important items in crystalline silicon PV research are to lower the (module) cost and to overcome the expected silicon shortage [1]. The use of thinner silicon wafers can attribute to both items, because the required amount of silicon per W_p decreases assuming that the solar cell efficiency and the production yield are not adversely affected by the use of thinner wafers.

In this work we will first investigate the influence of thickness on the output of solar cells made using standard industrial processing. Next we estimate which efficiency gain can be obtained when a better surface passivation is realised. Finally we determine possible causes for the limited rear surface passivation and we present methods to improve the Back Surface Field (BSF).

EXPERIMENTAL METHODS

To investigate the effect of the wafer thickness on the solar cell characteristics 10 sets of 100 cm^2 multicrystalline silicon wafers have been processed using standard industrial techniques. First, after a saw damage etch using NaOH, the emitter was diffused in a belt furnace. Next, the phosphorus glas was removed using 25% HF and a MW RPECVD SiN_x anti reflection coating was applied [2]. Finally, the front side (Ag) and rear side (Al) metallisation were screen printed and fired in one single step in an IR heated belt furnace. Each set consisted of 8 neighbouring wafers. Within each set, the thickness of the wafers before the saw damage etch ranged from 150 µm to 325 µm with steps of 25 µm.

The IV characteristics of all cells were measured. The reflectance, the spectral response and the Al doping profile were measured on selected cells. To determine the significance of the observed trends a two factor analysis of variance was performed using the computer program Statgraphics Plus version 5 [3,4]. Produced solar cells were modelled with PC1D version 4.5 [5] to identify what limits the efficiency and to estimate the possible efficiency gain.

To investigate the influence of the firing conditions on the effective surface recombination velocity we measured the effective lifetime of a 200 µm thick wafer using the QSSP method [6]. First, the lifetime was measured with one surface passivated by an Al-BSF and the other surface passivated by a highly doped emitter. Second, the lifetime was measured again after removal of the emitter and the Al-BSF using chemical etching and both surfaces passivated by a PECVD SiN_x coating. With the known effective surface recombination velocity of the highly doped emitter, the effective surface recombination velocity of the applied Al-BSF can be determined from eq (3) [7]:

$$\frac{1}{\tau_{BSF}} = \frac{1}{\tau_{bulk}} + \frac{(J_{0,front}+J_{0,back})(n_a-\Delta n_a)}{qn_i 2W} \qquad \text{eq. (1)}$$

$$\frac{1}{\tau_{SiNx}} = \frac{1}{\tau_{bulk}} + \frac{2S}{W} \qquad \text{eq. (2)}$$

Subtracting equation (2) from equation (1), assuming that S ≈ 0 cm/s in the nitride coated system and using S instead of J_0 gives:

$$\frac{1}{\tau_{BSF}} - \frac{1}{\tau_{SiNx}} = \frac{S_{eff,front}+S_{eff,back}}{W} \qquad \text{eq. (3)}$$

τ_{SiNx} and τ_{BSF} are the QSSP lifetimes with the SiN_x passivation and the Al-BSF/emitter passivation respectively. To determine the significance of the observed trends we also performed a two factor analysis of variance on these results.

SOLAR CELL EFFICIENCY AND WAFER THICKNESS

In Table 1 the mean value of the main electrical parameters of the solar cells are given. Within the 95 % confidence limit, both J_{sc} and V_{oc} are independent of the wafer thickness for wafers thicker than 200 µm. For thinner wafers the decrease in J_{sc} becomes statistically significant. The experimental results prove that wafers as thin as 200 µm can be processed without loss in efficiency.

To explain the results, cells were modelled with PC1D. The surface recombination, the minority carrier diffusion length in the bulk, the diffusion length in the BSF and the surface recombination velocity have been determined by iteration until the measured IQE of the 325 µm thick wafer and the J_{sc} and the V_{oc} of all wafers were fitted well by PC1D. Some parameters were fixed on their measured experimental values (see Table 2). In Figure 1 and Figure 2 the measured values and the best fit are shown. To obtain these fits, a minority carrier diffusion length of 300 µm in the bulk and of 0.4 µm in the Al-BSF had to be assumed. For the front surface recombination velocity a value of $1{\cdot}10^6$ cm/s has been found. The effect of the BSF is equivalent to an effective rear side recombination velocity of about 4200 cm/s which is very high.

Table 1: Cell results of neighbour cells with varying thickness. Errors show 95 % confidence limit.

W µm	J_{sc} mA/cm^2	V_{oc} mV	FF %	η %
325	30.2 ± 0.2	601 ± 2	74 ± 1	13.5 ± 0.2
300	29.8 ± 0.2	601 ± 2	74 ± 1	13.3 ± 0.2
275	30.2 ± 0.2	602 ± 2	73 ± 1	13.3 ± 0.2
250	30.0 ± 0.2	601 ± 2	74 ± 1	13.4 ± 0.2
225	29.9 ± 0.2	602 ± 2	75 ± 1	13.4 ± 0.2
200	29.7 ± 0.2	600 ± 2	75 ± 1	13.3 ± 0.2
175	29.3 ± 0.2	599 ± 2	73 ± 1	12.9 ± 0.2
150	29.1 ± 0.2	597 ± 3	71 ± 1	12.4 ± 0.2

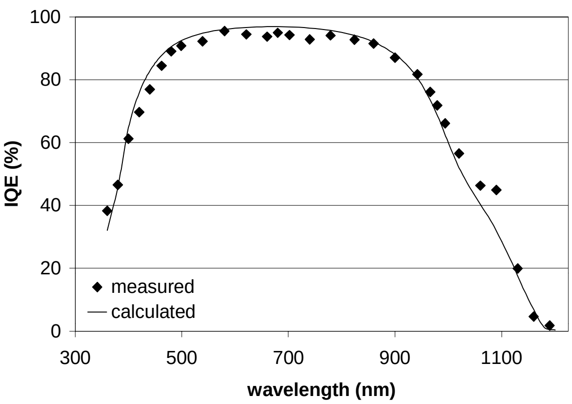

Figure 1: IQE data for 325 µm wafer. Solid curves are calculated using PC1D: best fits are obtained for L_{bulk} = 300 µm; L_{BSF} = 0.4 µm, $S_{front} = 10^6$ cm/s

Table 2: Experimental values used in PC1D calculations.

	value	measured by
front metal coverage	9 %	visually
emitter profile		Stripping Hall
[B] base	$1.5{\cdot}10^{16}$ at B / cc	ECV
[B] BSF	$5{\cdot}10^{18}$ at B / cc	ECV
thickness BSF	9 µm	ECV
rear reflection	78 %	ref. [8]
thickness ARC	71 nm	reflection
refractive index ARC	2.2	reflection

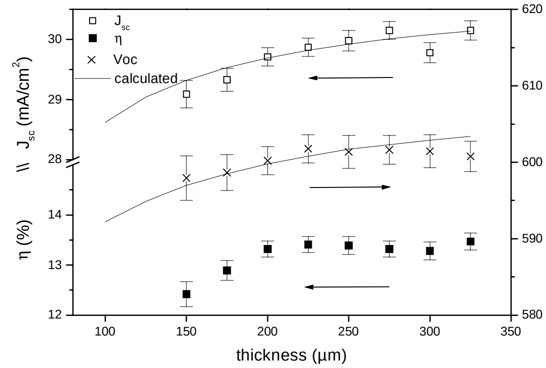

Figure 2: J_{sc} and V_{oc} and η as a function of the wafer thickness. Error bars show 95% confidence limits. Solid curves are calculated with PC1D using the parameters given in Table 2 and $S_{front} = 10^6$ cm/s, L_{BSF} = 0.4 µm, and L_{bulk} = 300 µm. N.B. L_{BSF} = 0.4 corresponds to $S_{eff.back}$ = 4200 cm/s.

BSF IMPROVEMENT

Modelling

We modelled the influence of the effective recombination velocity at the rear side on the efficiency of a 200 µm thick solar cell to determine what the influence is of the rear surface passivation (Figure 3). The PC1D parameters obtained in the previous section were used. An efficiency gain of 1.1 % absolute can be obtained when Srear is improved from 4200 cm/s to 200 cm/s. For comparison, the influence of the front side recombination velocity is also shown, which could improve the efficiency by 0.8% maximally.

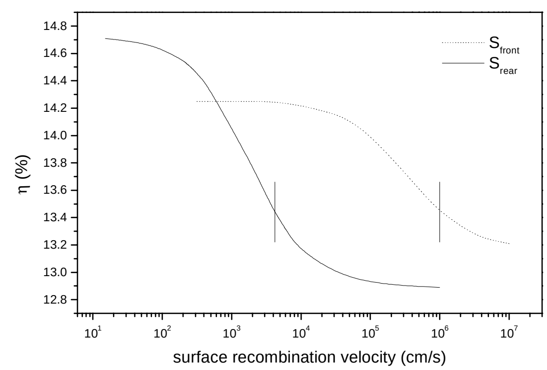

Figure 3: Effect of surface passivation on the efficiency of a 200 µm thick wafer. The curves are calculated with PC1D using the parameters given in Table 2 and L_{bulk} = 300 µm, $S_{front} = 10^6$ cm/s (in calculating the dependence of S_{rear}) and S_{rear} = 4200 cm/s (in calculating the dependence of S_{front}). The vertical markers indicate the experimental surface recombination velocities.

The BSF can be improved by increasing the dopant level or BSF thickness [9], increasing the heat-up rate in the alloying process [10], or decreasing the cool-down rate of the crystallisation process [11]. We investigated the effect of dopant level, impurity content of the aluminium and the firing conditions (temperature and belt speed).

BSF dopant concentration

We increased the dopant concentration of the BSF by adding a small amount of boron to the used Al paste. Figure 4 shows that this does indeed increase the dopant concentration in the BSF. However, we have not observed an increase in the internal quantum efficiency for long wavelengths of produced solar cells. This shows that the rear surface passivation has not been improved.

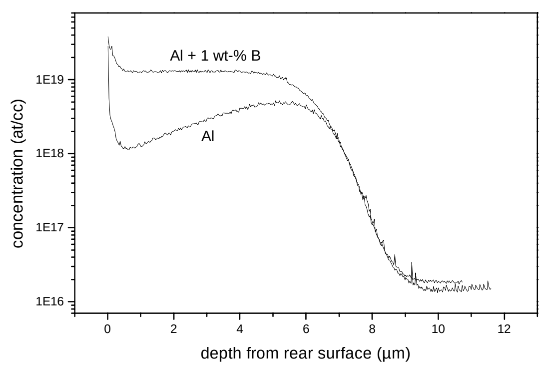

Figure 4: Dopant concentration of a BSF made with and without a boron addition to the Al-paste. Measured using ECV.

Aluminium purity

The very low minority carrier lifetime is not caused by the aluminium dopant itself. Highly Al doped silicon layers with diffusion lengths of over 40 µm have been prepared with liquid phase epitaxy by others [12]. The low lifetime could neither be attributed to the purity of the used aluminium. Cells in which the Al-BSF was made using sputtered high purity Al showed the same very low lifetime in the Al-BSF.

Firing conditions

To investigate the influence of the firing conditions on the quality of the BSF, BSFs were made at 3 different belt speeds and at 4 different firing temperatures. Differences in bulk diffusion length can be attributed to the processing parameters because neighbouring wafers have been used. Both the heat-up and cool-down rate are changed by changing the temperature or the belt speed. Besides that, higher temperatures will result in a higher dopant concentration and a thicker BSF. In Table 3 andTable **4** and Figures 5 and 6 the estimated bulk lifetime and the effective rear surface recombination velocity for the various firing conditions are presented. In this experiment, hydrogen passivation is absent because no firing with an SiN_x coating has been done. This limits the value of τ [2].

Table 3: Bulk lifetime (µs) for various Al-BSF firing conditions estimated using eq. (3). Belt speed and temperature settings are given as a deviation from the default solar cell processing conditions

belt speed / temp	-10"	-5"	0”
-60 °C	4.3	5.3	4.5
-40 °C	8.2	9.2	7.8
-20 °C	7.3	11.9	10.9
0 °C	7.2	10.4	10.8

Table 4: Effective rear surface recombination velocity (cm/s) for various Al-BSF firing conditions estimated using eq. (3). Belt speed and temperature settings are given as a deviation form the default solar cell processing conditions.

belt speed / temp	-10”	-5”	0”
-60 °C	400	1600	2200
-40 °C	1600	2500	2800
-20 °C	1500	2500	2300
0 °C	1500	2600	2700

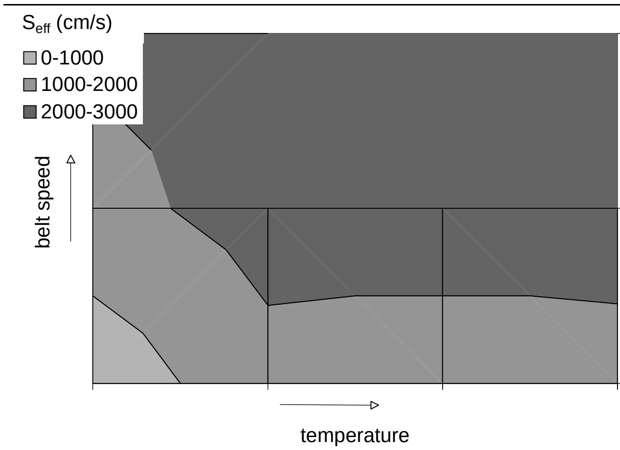

Figure 5: Contour plot of the effective rear surface recombination velocity of an Al-BSF as a function of belt speed and firing temperature.

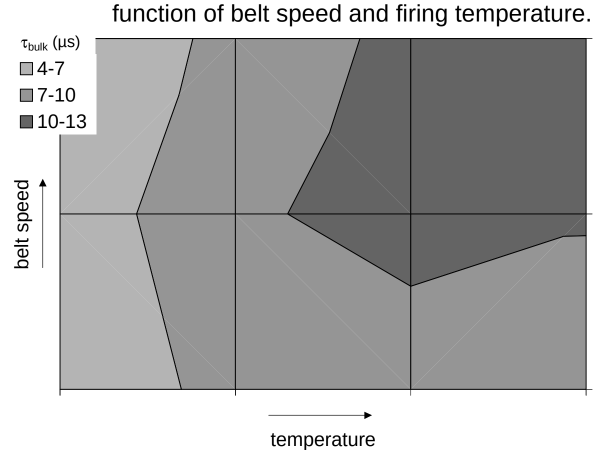

Figure 6: Contour plot of the minority carrier bulk lifetime as a function of belt speed and firing temperature.

A large minority carrier lifetime and a low rear surface recombination velocity are inversely related as is shown by comparing Figure 5 and Figure 6. A good surface passivation is obtained at a low belt speed and a low firing temperature, while a good bulk quality is obtained at a high belt speed and a high firing temperature. Statistical analysis of the results revealed that within the 95 % confidence limit, the belt speed has no significant influence on the bulk quality.

The trend in effective surface passivation can be explained by the crystallisation rate. A low belt speed and a low firing temperature both result in a lower crystallisation rate of the BSF, and thus in a better material quality in the crystallised layer. This minimises the deterioration of the minority carrier diffusion length in the BSF.

The improvement in the bulk material quality probably results from aluminium gettering. Al gettering is a diffusion limited process [9], so it is favoured by a high temperature. However, a low belt speed would also favour Al gettering, but the statistical analysis shows that the belt speed has no significant influence on the bulk quality. Figure 6 even suggests that a low belt speed might have a negative influence on the bulk properties. This probably is the result from a balance between gettering and thermal degradation.

Bulk gettering takes place in the high temperature section of the firing, while BSF crystallisation takes place at the ramp-down. Therefore, it should be possible to combine a good bulk quality and a good rear surface passivation in one single Al-BSF firing step. Experiments to combine the high heat-up rate and high temperature with a low cool-down rate are underway.

CONCLUSION

Wafers as thin as 200 µm can be processed into solar cells without loss of efficiency compared to 330 µm thick wafers.

The effective rear side recombination velocity of the BSF is about 4200 cm/s and it is limited by the short minority carrier diffusion length of the applied Al BSF. Applying a good rear surface passivation can result in an efficiency increase of more than 1 % absolute.

The low minority carrier diffusion length of the Al-BSF is not caused by the aluminium or by impurities in the aluminium. Our experiments show that the most likely explanation is the poor crystallinity of the Al-BSF due to the fast cooling during the metallisation firing.

The effective rear side recombination velocity can be decreased to about 500 cm/s by using different firing conditions.

ACKNOWLEDGEMENTS

This work has been financially supported by the NOZ-PV programme of the Netherlands Agency for Energy and the Environment (Novem).

We thank Ron Sinton for his advice in extracting τ_{bulk} and S_{rear} from the measurements.

REFERENCES

[1] H. Aulich, F.W. Schulze, "Crystalline silicon feedstock for solar cells", *Prog. Photovolt: Res. Appl.*, **10**, 2002, pp. 141-147.

[2] W.J. Soppe. B.G. Duijvelaar, S.E.A. Schiermeier, A.W. Weeber, A. Steiner, F.M. Schuurmans, "A high throughput PECVD reactor for depositing of passivating SiN layers", Sixteenth EU PVSEC, 2000, pp. 1420-1423.

[3] A.W. Weeber, W.C. Sinke, "Statistical analysis for solar cell research", *Twenty-fifth IEEE PVSC,* 1996, pp. 565-567.

[4] http://www.statgraphics.com

[5] P.A. Basore, D.A. Clugston, "PC1D version 4 for windows: from analysis to design", *Twenty-fifth IEEE PVSC,* 1996, pp. 377-381.

[6] R.A. Sinton, "Quasi-stead-state photoconductance, a new method for solar cell material an device characterization" , *Twenty-fifth IEEE PVSC,* 1996, pp. 457-460

[7] R.A. Sinton, A. Cuevas, "Contactless determination of current-voltage characteristics and minority-carrier lifetimes in semiconductors from quasi-steady-state photoconductance data." *Appl. Phys. Lett*. **69**(17), 1996, pp. 2510-2512.

[8] C.J.J. Tool, A.R. Burgers, P. Manshanden, A.W. Weeber, B.H.M. van Straaten, "Influence of wafer thickness on the performance of multicrystalline Si solar cells; an experimental study", *Prog. Photovolt. Res. Appl.* **10**, 2002, pp. 279-291.

[9] P. Lölgen, "Surface and volume recombination in silicon solar cells. PhD Thesis: Utrecht University, 1995.

[10] S. Narasimha, A. Rohatgi, A.W. Weeber, "An optimized rapid aluminium back surface field technique for silicon solar cells" *IEEE Trans. Electron Devices* **46**, 1999, pp. 1363-1369.

[11] P. Lölgen, C.Leguijt, J.A. Eikelboom, R.A. Steeman, W.C. Sinke, L.A. Verhoef, P.F.A. Alkemade. E. Algra "Aluminium back-surface field doping profiles with surface recombination velocities below 200 cm/s." *Twenty-third IEEE PVSC*, 1993, pp. 236-242.

[12] T.H. Wang, T.F. Ciszek, C.R. Schwerdtfeger, H. Moutinho, R. Matson, "Growth of silicon thin layers on cast MG-Si from metal solution for solar cells." *Solar Energy Mater. Solar Cells* **41/42**, 1996, pp. 19-30.